Volume 13, Issue 1, Page 142-151, 2024 https://doi.org/10.46810/tdfd.1362191 Research Article

BİNGÖL UNIVERSITY

Türk Doğa ve Fen Dergisi
Turkish Journal of Nature and Science
www.dergipark.gov.tr/tdfd

Developing a Regression Model for Predicting the Seismic Input Energy of RC Buildings Using 6 February 2023 Kahramanmaraş Earthquake

Bilal BALUN[1*]

[1] Bingöl University, Centre for Energy the Environment and Natural Disasters and Department of Architecture, Bingöl, Türkiye
Bilal BALUN ORCID No: 0000-0003-0906-4484

**Corresponding author: bbalun@bingol.edu.tr*

(Received: 18.09.2023, Accepted: 19.03.2024, Online Publication: 26.03.2024)

Keywords
Kahramanmaraş earthquake, Input energy, Multiple regression, Correlation

Abstract: Energy-based seismic analysis and structural design require understanding the seismic input energy response of reinforced concrete buildings subjected to strong ground motions. Thus, calculating and predicting input energies becomes of great importance. The object of this study is to introduce a regression model for predicting the seismic input energies of reinforced concrete buildings using the 6 February 2023 Kahramanmaraş/Pazarcık earthquake which devastating damage occurred. For this purpose, three regular 3, 6 and 9-storey residential reinforced concrete buildings are designed. Input energy response histories of buildings subjected to a set of horizontal acceleration histories of 67 stations of the February 6 Kahramanmaraş/Pazarcık earthquake were obtained. Subsequently, the ground motion parameters were used to estimate the input energies. It was revealed that acceleration-based parameters generally had better consequences than velocity-based parameters in low periods, while the opposite was the case in high periods. In 3, 6 and 9-storey buildings, the highest correlation coefficients were obtained in I_c (0.91), ASI (0.83) and VSI (0.73) parameters, respectively. This study proposed new equations in which multiple ground motion parameters are combined to better reflect input energy from a single parameter. In the multi regression where all parameters were used, correlation values (R^2) of 0.94, 0.85 and 0.77 were determined, respectively, according to the number of floors of the buildings. As the height and period of the buildings increase, the multiple linear regression coefficient decreases and the estimation of input energy becomes difficult with the ground motion parameters.

6 Şubat 2023 Kahramanmaraş Depremi Kullanılarak Betonarme Binaların Sismik Giriş Enerjisinin Tahmin Edilmesine Yönelik Regresyon Modeli Geliştirilmesi

Anahtar Kelimeler
Kahramanmaraş depremi, Sismik giriş enerjisi, Çoklu regresyon, Korelasyon

Öz: Enerji bazlı sismik analiz ve yapı tasarımı, kuvvetli yer hareketlerine maruz kalan betonarme binaların sismik giriş enerji tepkisinin anlaşılmasını gerektirir. Bu nedenle giriş enerjilerinin hesaplanması ve tahmin edilmesi büyük önem kazanmaktadır. Bu çalışmanın amacı, yıkıcı hasarların meydana geldiği 6 Şubat 2023 Kahramanmaraş/Pazarcık depremini kullanarak betonarme binaların sismik giriş enerjilerini tahmin etmeye yönelik bir regresyon modeli ortaya koymaktır. Bu amaçla 3, 6 ve 9 katlı üç adet düzenli konut betonarme bina tasarlanmıştır. 6 Şubat Kahramanmaraş/Pazarcık depreminin 67 istasyonunun bir dizi yatay ivme geçmişine tabi tutulan binaların giriş enerji tepki geçmişleri elde edildi. Daha sonra giriş enerjilerini tahmin etmek için yer hareketi parametreleri kullanıldı. Düşük periyotlarda ivmeye dayalı parametrelerin genellikle hıza dayalı parametrelere göre daha iyi sonuçlara sahip olduğu, yüksek periyotlarda ise bunun tam tersi olduğu ortaya çıktı. 3, 6 ve 9 katlı binalarda en yüksek korelasyon katsayıları sırasıyla I_c (0,91), ASI (0,83) ve VSI (0,73) parametrelerinde elde edildi. Bu çalışma, tek bir parametreden gelen girdi enerjisini daha iyi yansıtmak için birden fazla yer hareketi parametresinin birleştirildiği yeni denklemler önermiştir. Tüm parametrelerin kullanıldığı çoklu regresyon modelinde binaların kat sayısına göre sırasıyla 0,94, 0,85 ve 0,77 korelasyon değerleri (R^2) belirlendi. Binaların yüksekliği ve periyodu arttıkça çoklu doğrusal regresyon katsayısı azalmakta ve yer hareketi parametreleri ile girdi enerjisinin tahmini zorlaşmaktadır.

1. INTRODUCTION

Türkiye has been affected by many devastating earthquakes throughout its history, as it is a seismically active region. [1]. Türkiye experienced massive destruction during the earthquake couple which occurred, at nine-hour intervals in Pazarcık (M_w 7.7) and Elbistan (M_w 7.6) on February 2023 [2]. On February 6, the accumulated energy of the Eastern Anatolian Fault Zone (EAFZ) was released by a tearing mechanism from north to south, just like a zipper [3]. The successive occurrence of these earthquakes caused property damage and loss of life three times than of the 1999 Marmara earthquake [4]. Balun [5] stated this situation as the seismic energy intensity of the February 6 Kahramanmaraş earthquake was much greater than previous earthquakes in Türkiye after the invention of devices. After these two significant earthquakes, in 11 different provinces more than 50,000 people lost their lives and caused many buildings to collapse or significant structural damage [6]. Previous studies pointed out the damage of the many types of structures. Destructions and damages were observed, especially in reinforced concrete buildings, which constitute the majority of the building stock of the region, and it was stated that poor materials, workmanship quality, inadequate detailing and architectural design errors were the main factors of these damages [1,3,4,7–9]. Furthermore, masonry structures, mosques and minarets were also examined and damages due to structural defects were reported [2,6,10]. It has been understood that earthquake code design criteria and requirements are insufficient in some regions. Considering the very severe earthquake level, it is a striking result that the accelerations obtained from many stations exceed the response spectrum values estimated by Türkiye Building Earthquake Code (TBEC 2018) [4,10]. All these field observations have revealed that construction and design defects cause inevitable loss of life and property. It has also been emphasized that ground motions above the design spectrum values are another important cause of damage. Apart from the structural damage caused by buildings, examining the density distribution after these earthquakes through peak ground acceleration and estimation of actual loss of life and structural damage has contributed to the literature [11,12]. In addition to all the researches and assessments made, it is thought that the interpretation of the February 6 earthquakes through the estimation of the seismic input energies will be valuable in terms of understanding both the design approach and the destructive effects of these earthquakes.

Strong ground motions that have occurred in the world in recent years have caused serious damage to relatively many new buildings designed according to conventional force or displacement-based seismic methods. If the instance exists due to deficiencies in the seismic design code, it is further confirmation that force or displacement-based design does not result in reliable structural seismic design of building systems [13]. This situation has increased the importance of energy-based design. To overcome these problems, an alternative seismic analysis and design approach that takes into account the duration, frequency content and cumulative damage potential of ground motion, defined as energy-based seismic design, has been introduced by Housner [14].

Although earthquakes are quite irregular ground motions, the input energy passing through the structure is a very stable parameter. Part of the input energy passing through the structure by ground motion is distributed by the damping mechanism, while the other part is distributed by cyclic energy [15–17]. Energy-based methods are achieved by providing sufficient capacity to building elements compared to seismic demand. The basis of energy-based seismic design is that the loading effect of seismic excitation on structures can be interpreted not as separate forces or displacements, but as the product of both in terms of input energy. However, it is accepted by many authors that the loading history affects the cumulative damage in seismic excitations [18–21].

Energy and energy parameters are the most promising parameters for the design of structures exposed to moderate or severe earthquakes. In the energy-based design approach, the primary task is the precise calculation of the input energy. Practical prediction of seismic input energy of multi degree of freedom systems (MDOF) is quite essential, especially in terms of seismic-based design [22]. The damage potential of structures is not only affected by the characteristics of ground motion but is also a function of structural characteristics. With a similar approach, seismic input energy is also affected by both characteristics. The damage potential of structures is generally reflected by ground motion parameters such as peak ground acceleration (PGA), peak ground velocity (PGV) and peak ground displacement (PGD). Although PGA is widely used as a dominant parameter in the assessment of structural performance, some studies have shown that this parameter alone does not have a strong correlation with structural damage [23–25]. Correlations and relationships of ground motion parameters with seismic input energy can eliminate complex calculations. In support of this, many studies in the literature have found relationships between ground motion characteristics and structural damage [26–28]. However, in most studies, it has been difficult to establish strong relationships between damage potential and ground motion characteristics [16,29]. It is thought that evaluating more than one parameter together will provide advantages in seismic input energy estimation.

Unlike the studies conducted for the February 6 Kahramanmaraş earthquake, estimating the input energy that causes structural damage with ground motion parameters in this study is a different perspective in terms of seismic evaluation. For this purpose, this study aims to reveal a strong correlation with seismic input energy by taking into account multiple regression in which ground motion characteristics are considered together. Three regular residential reinforced concrete buildings with 3, 6 and 9 storeys were designed to

determine the relationships between seismic input energy and ground motion parameters. Input energy response histories of 3D-designed buildings subjected to a series of horizontal acceleration histories of 67 stations of the February 6 Pazarcık earthquake were obtained, and their correlations with seismic parameters were evaluated. Ultimately, seismic input energy will be predicted using the multiple regression analysis based on several parameters, such as acceleration, velocity, displacement, frequency and duration.

2. STRONG GROUND MOTION DATASET

The current study consists of 25 ground motion parameters to analyze the relationship with seismic input energy. In structural damage assessment, commonly used peak values alone do not lead to an understanding of the damage potential of strong ground motions to structures. Many other ground motion parameters can contribute to structural damage [30]. The seismic parameters given in Table 1 are classified according to acceleration, velocity, displacement, frequency and ground motion duration. Additionally, in this study, significant duration was considered to reveal the duration effect. The values of parameters used in the study are determined using the software SeismoSignal (2021) [31]. The relationship between a parameter and other parameters can be examined through correlation analysis. Additionally, multiple regression analysis was performed to reveal the relationship of multiple parameters with seismic input energy and equations were obtained for prediction.

Table 1. Seismic parameters

Type	Parameter	Definition	Formula
Acceleration-based	PGA	Peak ground acceleration	$PGA = \max\|a(t)\|$
	a_{RMS}	Root-mean-square of acceleration	$a_{RMS} = \sqrt{\frac{1}{t_{tot}}[a(t)]^2 dt}$
	I_a	Arias intensity	$I_a = \frac{\pi}{2g}\int_0^t a^2(t)dt$
	I_c	Characteristic intensity	$I_c = (a_{RMS})^{\frac{3}{2}}\sqrt{t_{tot}}$
	CAV	Cumulative absolute velocity	$CAV = \int_0^t a(t)dt$
	SMA	Sustained maximum acceleration	3rd largest peak in acceleration time history
	EDA	Effective Design Acceleration	Peak acceleration value above 9 Hz
	A_{95}	A_{95} Parameter	The acc. level below 95% of the total I_a
	SCAV	Standardized Cumulative Absolute Velocity	$SCAV = \sum_{i=1}^{n}(H(PGA) - 0.025)\int_{i-1}^{i}\|a(t)\|dt)$
	$S_{a,avg}$	Average Spectral Acceleration	$S_{a(T1\ldots TN)} = \left(\prod_{i=1}^{n} S_a(T_i)\right)^{1/n}$
	ASI	Acceleration spectrum intensity	$ASI = \int_{0.1}^{0.5} S_a(\xi = 0.05, T)dT$
Velocity-based	PGV	Peak ground velocity	$PGV = \max\|v(t)\|$
	v_{RMS}	Root-mean-square of velocity	$v_{RMS} = \sqrt{\frac{1}{t_{tot}}[v(t)]^2 dt}$
	SED	Specific energy density	$SED = \int_0^t [v(t)]^2 dt$
	SMV	Sustained maximum velocity	3rd largest peak in velocity time history
	MIV	Maximum Incremental Velocity	Acc. curve between two zero crossings of the accel.
	VSI	Velocity spectrum intensity	$VSI = \int_{0.1}^{2.5} S_v(\xi = 0.05, T)dT$
	HI	Housner intensity	$HI = \int_{0,1}^{2,5} PSV(\xi = 0{,}05, T)dT$
Disp.-based	PGD	Peak ground displacement	$PGD = \max\|d(t)\|$
	d_{RMS}	Root-mean-square of displacement	$d_{RMS} = \sqrt{\frac{1}{t_{tot}}[d(t)]^2 dt}$
	v_{max}/a_{max}	Peak velocity to acceleration ratio	v_{max}/a_{max}
Frequency-based	T_p	Predominant Period	The period at which the maximum spectral acc.
	T_m	Mean Period	$T_m = \frac{\sum C_i^2/f_i}{\sum C_i^2}$
Duration-based	$D_{5\text{-}95}$	Significant duration (5%-95%)	The time period over which total Arias Intensity is collected from 5% to 95%
	$D_{5\text{-}75}$	Significant duration (5%-75%)	The time period over which total Arias Intensity is collected from 5% to 75%

Analyzes were performed under the ground motion record set listed in Table 2 for the determined building models. Both horizontal components of the 67 station records of the 2023 Kahramanmaraş earthquake, which

occurred at 04:17 local time and had a magnitude of M_w 7.7, extracted from the AFAD database, were used. Furthermore, the coordinates of the stations, shear wave velocity (V_{s30}) of the soil and distance to epicenter values are also given. The selection criterion for ground motions is that the peak ground acceleration values of the records are greater than 0.1g, where g is the gravitational acceleration. In the analysis, acceleration records were used without spectrum matching. The aim is to reveal the relationships that are the subject of the article by using real ground motions of the Kahramanmaraş earthquake, which caused a lot of destruction and loss of life. In the intensity map in Figure 1 presented by AFAD [32], it is seen that ground motions greater than 0.1 g mostly occur in Hatay and Kahramanmaraş provinces and their surroundings.

Table 2. The properties of the selected earthquake records (February 6 Kahramanmaraş (M_w 7.7))

No	Station	City	District	Longitude	Latitude	V_{s30} (m/s)	R_{epi} (km)
1	120	Adana	Yumurtalık	35.790	36.770	439	125.25
2	125	Adana	Ceyhan	35.796	37.015	208	114.62
3	131	Adana	Saimbeyli	36.115	37.857	None	103.35
4	201	Adıyaman	Adıyaman	38.267	37.761	391	120.12
5	213	Adıyaman	Tut	37.930	37.797	None	96.48
6	2703	Gaziantep	Şahinbey	37.350	37.058	758	37.34
7	2704	Gaziantep	Nizip	37.802	37.009	721	74.10
8	2708	Gaziantep	İslahiye	36.648	37.099	523	40.77
9	2709	Gaziantep	İslahiye	36.670	37.129	555	37.45
10	2711	Gaziantep	Yavuzeli	37.560	37.317	None	45.88
11	2712	Gaziantep	Nurdağı	36.733	37.184	None	29.79
12	2714	Adıyaman	Besni	37.621	37.492	None	55.92
13	2715	Gaziantep	İslahiye	36.686	36.855	None	57.62
14	2716	Gaziantep	İslahiye	36.688	36.856	None	57.38
15	2717	Gaziantep	İslahiye	36.691	36.855	None	57.34
16	2718	Gaziantep	İslahiye	36.627	37.008	None	48.30
17	3112	Hatay	İskenderun	36.148	36.588	233	111.31
18	3115	Hatay	Belen	36.165	36.546	424	113.7
19	3116	Hatay	İskenderun	36.207	36.616	870	105.38
20	3123	Hatay	Antakya	36.160	36.214	470	143.00
21	3124	Hatay	Antakya	36.172	36.239	283	140.11
22	3125	Hatay	Antakya	36.133	36.238	448	142.15
23	3126	Hatay	Antakya	36.138	36.220	350	143.54
24	3129	Hatay	Defne	36.134	36.191	447	146.39
25	3131	Hatay	Antakya	36.163	36.191	567	144.98
26	3132	Hatay	Antakya	36.172	36.207	377	143.12
27	3133	Hatay	Reyhanlı	36.574	36.243	377	123.47
28	3134	Hatay	Dörtyol	36.205	36.828	374	90.29
29	3135	Hatay	Arsuz	35.883	36.409	460	142.15
30	3136	Hatay	Altınözü	36.247	36.116	344	148.38
31	3137	Hatay	Hassa	36.489	36.693	688	82.48
32	3138	Hatay	Hassa	36.511	36.803	618	71.70
33	3139	Hatay	Kırıkhan	36.414	36.584	272	96.19
34	3140	Hatay	Samandağ	35.950	36.082	210	165.82
35	3141	Hatay	Antakya	36.220	36.373	338	125.42
36	3142	Hatay	Kırıkhan	36.366	36.498	539	106.49
37	3143	Hatay	Hassa	36.557	36.849	444	65.13
38	3144	Hatay	Hassa	36.486	36.757	485	77.04
39	3145	Hatay	Kırıkhan	36.406	36.645	533	91.13
40	3146	Hatay	Belen	36.227	36.491	None	114.57
41	4404	Malatya	Pütürge	38.874	38.196	1380	190.02
42	4406	Malatya	Akçadağ	37.974	38.344	815	143.07
43	4408	Malatya	Doğanşehir	37.887	38.096	654	116.59
44	4611	Kahramanmaraş	Çağlayancerit	37.284	37.747	731	55.32
45	4612	Kahramanmaraş	Göksun	36.482	38.024	246	95.59

46	4613	Kahramanmaraş	Andırın	36.357	37.570	998	68.19
47	4614	Kahramanmaraş	Pazarcık	37.298	37.485	541	31.42
48	4615	Kahramanmaraş	Pazarcık	37.138	37.387	484	13.83
49	4616	Kahramanmaraş	Türkoğlu	36.838	37.375	390	20.54
50	4617	Kahramanmaraş	Onikişubat	36.838	37.375	574	38.04
51	4618	Kahramanmaraş	Onikişubat	36.872	37.600	715	37.84
52	4619	Kahramanmaraş	Onikişubat	36.866	37.587	545	36.73
53	4620	Kahramanmaraş	Onikişubat	36.898	37.586	484	35.48
54	4621	Kahramanmaraş	Dulkadiroğlu	36.929	37.593	714	35.42
55	4624	Kahramanmaraş	Onikişubat	36.918	37.536	280	29.73
56	4625	Kahramanmaraş	Dulkadiroğlu	36.982	37.539	346	28.40
57	4626	Kahramanmaraş	Onikişubat	36.915	37.575	317	33.89
58	4629	Kahramanmaraş	Türkoğlu	36.789	37.287	382	22.05
59	4630	Kahramanmaraş	Türkoğlu	36.789	37.287	347	21.89
60	4632	Kahramanmaraş	Türkoğlu	36.774	37.256	428	24.09
61	6303	Şanlıurfa	Siverek	39.329	37.752	986	208.12
62	6304	Şanlıurfa	Bozova	38.513	37.365	376	130.27
63	6305	Şanlıurfa	Haliliye	38.513	37.365	None	155.06
64	8002	Osmaniye	Bahçe	36.562	37.192	430	43.91
65	8003	Osmaniye	Osmaniye	36.269	37.084	350	72.18
66	8004	Osmaniye	Kadirli	36.098	37.380	426	84.20
67	NAR	Kahramanmaraş	Pazarcık	37.157	37.392	None	15.35

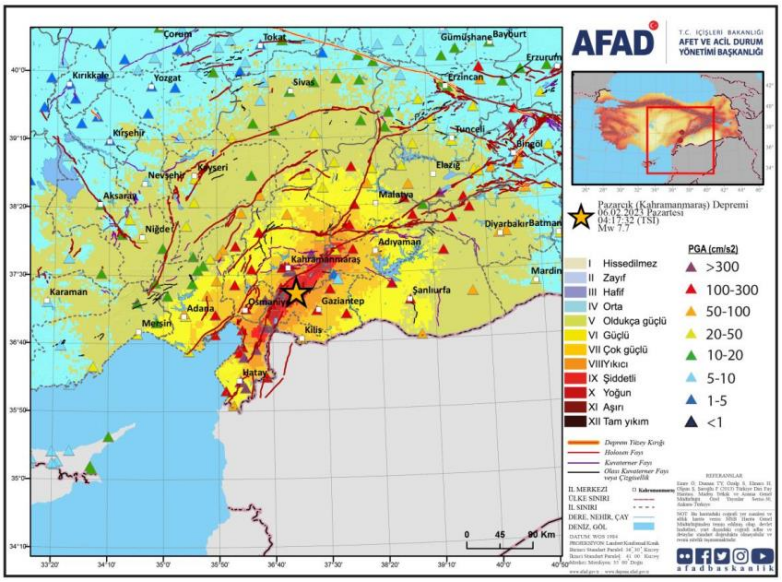

Figure 1. AFAD-RED intensity map of M_w 7.7 magnitude earthquake [32].

3. BUILDING MODEL

Building models with 3, 6 and 9 storeys are designed to represent the building inventory in the earthquake affected region. Even if buildings have different numbers of storey, buildings may have similar mass and period values due to their structural features. In this study, models were designed to provide diversity in terms of mass and period and correlations were examined. The plan and 3D model of the buildings in which nonlinear analyses were performed is given in Figure 2 and 3. The building structural system consists of frames with beams and columns but no shear walls. In the building model with four bays with a fixed width of 5.0 m, the storey height is 3.0 m on all storeys. Structural elements are designed by TBEC 2018 [33] code. The periods of the models representing low-rise, medium-rise and high-rise buildings are 0.40, 0.67 and 0.96 seconds, respectively. The floor/slab thickness is maintained at 0.15 m. The column dimensions are selected as 0.4x0.4 m, 0.5x0.5 m and 0.6x0.6 m for 3, 6 and 9-storey buildings, respectively. All beam dimensions are considered as 0.25x0.5 m. A rigid diaphragm model is assumed of the lateral response for the beam at each story level. The additional dead and live loads acting on floors are assumed to be 1 kN/m^2 and 2 kN/m^2, respectively. In the design and analysis process, the C25 grade concrete (28-day characteristic compressive strength of 25 N/mm^2) and the S420 grade of both longitudinal and transverse reinforcement steel (yield strength of 420 N/mm^2) are used for structural elements. Nonlinear time history analyses are

performed in ETABS V19 by using 134 different ground motion records of the 2023 Kahramanmaraş earthquake.

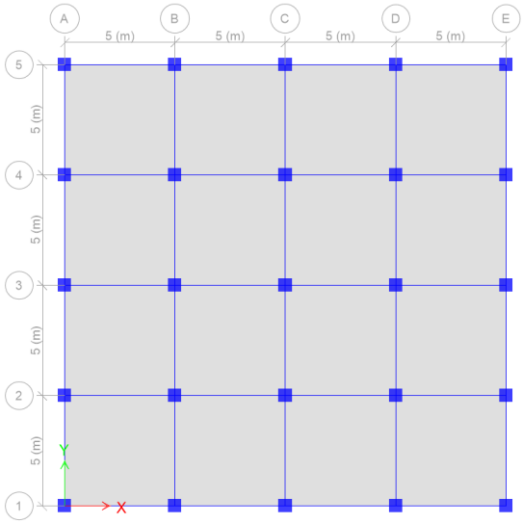

Figure 2. Plan of building models

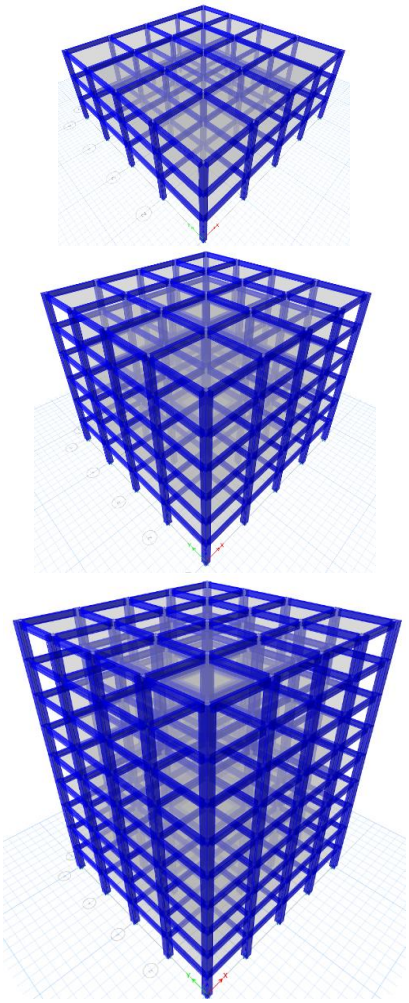

Figure 3. 3D models of buildings (3, 6 and 9-storey)

4. RESULTS AND DISCUSSIONS

Nonlinear time-history analyses were performed with 134 different acceleration records from 67 stations, and seismic input energies were obtained for each building model. Figure 4 presents the stations where the greatest input energy transmitted to 3, 6 and 9-storey buildings occurs and the graph of this energy change. First of all, the maximum input energies for each building model were calculated with the station data of the 2023 Kahramanmaraş/Pazarcık earthquake. Among 67 stations, the maximum input energies for 3, 6 and 9-storey buildings were obtained in Kahramanmaş/Pazarcık, Hatay/Defne and Hatay/Antakya, respectively. This result shows that low-period structures in Kahramanmaraş and high-period structures in Hatay were exposed to more input energy during the earthquake. Increasing seismic input energy may also increase the damage potential, depending on the building features.

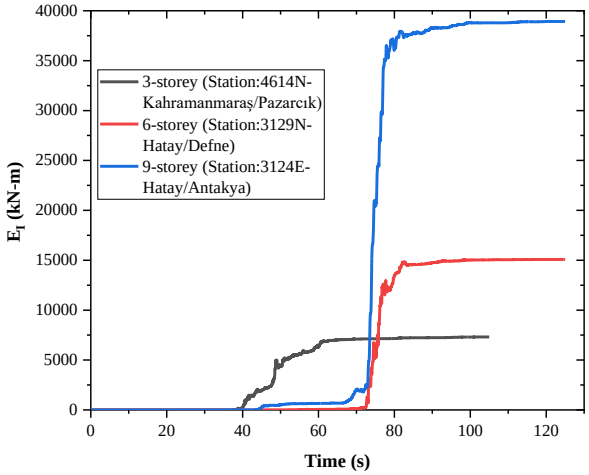

Figure 4. Input energies of 3, 6 and 9-storey RC buildings

In order to make a more accurate assessment, input energy values per unit mass (E_I/m) were obtained and buildings with different storey numbers were compared for 4 stations (Figure 4). These stations are among the stations where the highest acceleration values were obtained in the Pazarcık earthquake. E_I/m values in Kahramanmaraş, where the highest acceleration ground motion occurs (2.43 g), again show that buildings with low periods have to deal with more seismic energy. The same situation was effective in 6-storey buildings in Hatay (station 3129 and 3135) and 9-storey buildings in Gaziantep (station 2708). Hatay and Kahramanmaraş data in Figure 5 supports the results in Figure 4. At station 4614, less input energy was transferred per unit mass in structures with higher periods.

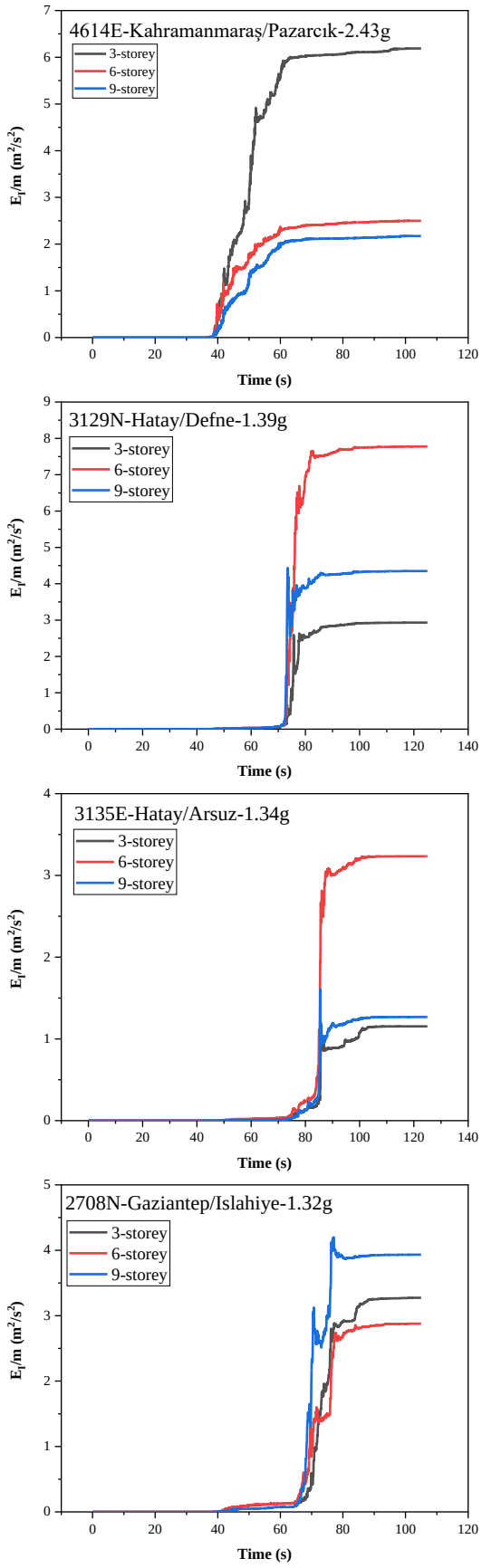

Figure 5. E_I/m values of stations (4614, 3129, 3135, 2708) for 3, 6 and 9-storey buildings

The ground motion parameters given in Table 1 for each station were obtained by SeismoSignal. Correlation analyses of the proposed ground motion parameters were performed with the Pearson correlation coefficient matrix (Equation 1). In this equation, xi and yi indicate the correlation parameters, $\bar{x}$ and $\bar{y}$ indicate the mean values of x_i and y_i, respectively. The correlation coefficient, a dimensionless quantity of variance, is commonly used and ranges from -1 to +1.

$$R = \frac{\sum(x_i - \bar{x})(y_i - \bar{y})}{\sqrt{\sum(x_i - \bar{x})^2 (y_i - \bar{y})^2}} \quad (1)$$

The bolded parameters in Table 3 indicate the first 6 highest correlation values in each parameter classification. While ground motion parameters are mostly positively correlated with seismic input energy, significant durations and some frequency-based parameters have a negative correlation. Displacement-based parameters were not among the parameters with the highest correlation. In 3, 6 and 9-storey buildings, the highest coefficients were obtained in I_c (0.91), ASI (0.83) and VSI (0.73) parameters, respectively. It has been determined that displacement-based, frequency-based and duration-based parameters have weaker relationships with input energy. In the correlation assessment, only input energy and one ground motion parameter were taken into account.

Table 3. Correlation coefficients (R) of ground motion parameters with input energy

Type	Parameter	3-storey	6-storey	9-storey
Acceleration-based	PGA	0.86	0.74	0.55
	a_{RMS}	**0.90**	0.72	0.57
	I_a	**0.88**	0.56	0.42
	I_c	**0.91**	0.66	0.51
	CAV	0.87	0.69	0.55
	SMA	**0.90**	0.73	0.54
	EDA	0.83	**0.78**	0.58
	A_{95}	0.86	**0.74**	0.55
	SCAV	**0.88**	0.68	0.54
	$S_{a.avg}$	0.54	**0.78**	**0.72**
	ASI	**0.88**	**0.83**	0.57
Velocity-based	PGV	0.46	0.65	0.6
	v_{RMS}	0.41	0.59	0.64
	SED	0.38	0.59	**0.7**
	SMV	0.51	0.66	**0.66**
	MIV	0.43	0.69	**0.67**
	VSI	0.53	**0.77**	**0.73**
	HI	0.49	**0.74**	**0.72**
Disp.-based	PGD	0.28	0.45	0.47
	d_{RMS}	0.38	0.44	0.47
	v_{max}/a_{max}	-0.27	-0.09	0.00
Freq.-based	T_p	-0.07	0.12	0.35
	T_m	-0.19	0.03	0.20
Dur.-based	D_{5-95}	-0.28	-0.29	-0.26
	D_{5-75}	-0.25	-0.28	-0.27

Figure 6 shows the changes in the correlation of acceleration-based, velocity-based and displacement-

based parameters. Figure 6a indicates that the correlation values in acceleration-based parameters decrease as the number of storey increases. Only the data obtained from the $S_{a,avg}$ parameter are excluded from this situation. Figure 6b explains that velocity-based parameters are generally more effective in buildings with high periods. Velocity-based parameters used in input energy estimation of low-period structures make their estimation more difficult. When both graphs in Figure 6 are examined, it is determined that acceleration-based parameters have a higher correlation with mean input energies than velocity-based parameters. The highest correlation occurs between the I_c-3-storey building and the lowest correlation between the PGD-3 storey building.

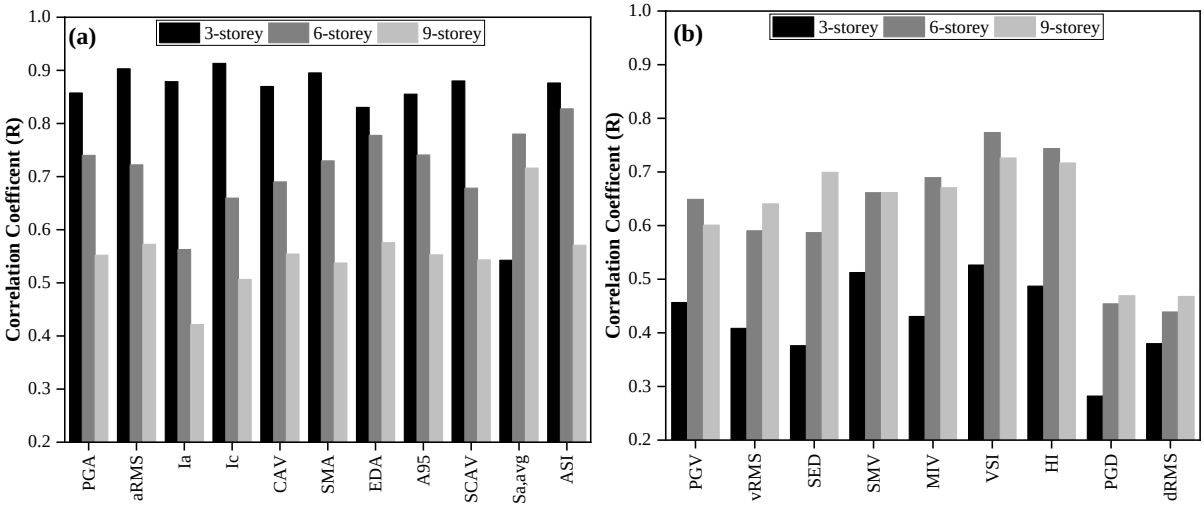

Figure 6. Correlation coefficients (R) of parameters with input energy (a) acceleration-based parameters, (b) velocity and displacement-based parameters

Table 4 contains the parameters with the highest correlation with seismic input energy for 3, 6 and 9-storey buildings. It has been determined that seismic input energy and acceleration-based parameters (a_{RMS}, I_a, I_c, ASI, SCAV, SMA) are in higher correlation in low-period structures. This situation changes as the period of the structure increases and as a result, the correlation relationship shifts towards velocity-based parameters (VSI, HI, SED, SMV, MIV). In many studies, it has been stated that peak ground motion parameters and acceleration-based parameters are in high correlation with demand variables in short-period structures [34–37]. In structures with intermediate periods, the input energy is closely related to both acceleration-based (ASI, A_{95}, SA, EDA) and velocity-based parameters (VSI, HI). a_{RMS}, ASI and VSI parameters reflect the input energy potential as the best single parameter for 3, 6 and 9-storey buildings, respectively.

Table 4. Predominant parameters for 3, 6 and 9-storey buildings

	3-storey	6-storey	9-storey
Predominant Parameters	a_{RMS}	ASI	VSI
	I_a	VSI	HI
	I_c	HI	SED
	ASI	A_{95}	SMV
	SCAV	SA	MIV
	SMA	EDA	SA

The method used to explain the cause-effect relationships between two or more independent variables affecting a variable with a model and to determine the effect levels of these independent variables is called multiple regression analysis. In this study, parameters used for multiple linear regression analysis define amplitude, frequency, and duration characteristics of ground motion. Predictive relationships are developed with multiple variables. Multiple regression analysis has been executed and performed for 25 ground motion parameters (GMP). The determinant coefficient (R^2), which expresses the degree of closeness to reality of the multiple regression where the dependent variable is input energy, is detailed in Table 5. Two different models were considered in this assessment. The first one expresses the multiple regression developed with the 6 ground motion parameters with the highest correlation value, while the second one covers all (25) ground motion parameters. Higher correlation values were obtained in the approach where all ground motion parameters were taken into account. Additionally, the highest R^2 values emerged for both models in low-period structures. As the building period increases, differences occur between the actual values in the calculation and the estimated values. As a result of linear regression analyses performed, equations 2, 3 and 4 were derived separately for 3, 6 and 9-storey buildings, respectively. The number of variables has been reduced to easily calculate the amount of input energy in the equations with fewer parameters (the first 6 GMPs).

Table 5. Correlation (R) and determinant (R^2) coefficients of GMP's

	6 GMP		All (25) GMP	
	R	**R^2**	**R**	**R^2**
3-storey	0,93	0,87	0,97	0,94
6-storey	0,87	0,76	0,92	0,85
9-storey	0,75	0,56	0,88	0,77

$$E_I(m^2/s^2) = -0.151 - 6.796a_{RMS} - 0.060I_a + 15.154I_c + 1.682ASI - 0.166SCAV - 1.282SMA \quad (2)$$

$$E_I(m^2/s^2) = -0.449 + 3.198ASI + 0.013VSI - 0.015HI + 0.012A_{95} + 3.048S_a - 1.350EDA \quad (3)$$

$$E_I(m^2/s^2) = -0.351 + 0.023VSI - 0.019HI + 7.6E^{-0.5}SED - 0.001SMV - 0.001MIV + 0.184S_a \quad (4)$$

5. CONCLUSION

In this study, input energy estimation for the devastating 6 February 2023 Kahramanmaraş earthquake was carried out and which parameters were highly correlated in which periods were revealed. As a result of the analyses of the structures, it is shown that the low-period structures in Kahramanmaraş and the high-period structures in Hatay are exposed to more input energy during the earthquake. It is worth noting that only structures with limited period values were analyzed. It has been found that acceleration-based parameters generally have better results than velocity-based parameters in low periods, and the opposite occurs in high periods. This study also proposed new regression equations in which multiple ground motion parameters are combined to better reflect input energy from a single parameter. With multiple linear regression analysis, a strong relationship between ground motion parameters and input energy was detected in low-period structures, and it was revealed that it was easier to estimate input energy with ground motion parameters in such structures for this earthquake. There is less difference between the coefficients of the two regression models proposed for low-period structures. However, to provide higher correlations in future studies, the database should be expanded, that is, more earthquake ground motion data should be used. The relationship between seismic parameters and input energies is also affected by the use of regression types. By accurately calculating and/or estimating input energies, damage indices and input energies can be more closely correlated in practice. Additionally, results can be obtained as to which earthquake parameters are more effective for a certain building stock. In subsequent studies, it is suggested that the relationships between strong ground motion parameters and input energy transmitted to the structure should be developed in irregular buildings.

REFERENCES

[1] Zengin B, Aydin F. The Effect of Material Quality on Buildings Moderately and Heavily Damaged by the Kahramanmaraş Earthquakes. Appl Sci 2023;13.

[2] Işık E. Structural Failures of Adobe Buildings during the February 2023 Kahramanmaraş (Türkiye) Earthquakes. Appl Sci 2023;13.

[3] Avcil F, Işık E, İzol R, Büyüksaraç A, Arkan E, Arslan MH, vd. Effects of the February 6, 2023, Kahramanmaraş earthquake on structures in Kahramanmaraş city. 2023.

[4] Ozturk M, Arslan MH, Korkmaz HH. Effect on RC buildings of 6 February 2023 Turkey earthquake doublets and new doctrines for seismic design. Eng Fail Anal 2023;153:107521.

[5] Balun B. Assessment of seismic parameters for 6 February 2023 Kahramanmaraş earthquakes. Struct Eng Mech 2023;88:117–28.

[6] Işık E, Avcil F, Büyüksaraç A, İzol R, Hakan Arslan M, Aksoylu C, vd. Structural damages in masonry buildings in Adıyaman during the Kahramanmaraş (Turkiye) earthquakes (Mw 7.7 and Mw 7.6) on 06 February 2023. Eng Fail Anal 2023;151.

[7] Ozkula G, Dowell RK, Baser T, Lin JL, Numanoglu OA, Ilhan O, vd. Field reconnaissance and observations from the February 6, 2023, Turkey earthquake sequence. vol. 119. Springer Netherlands; 2023.

[8] Ozturk M, Arslan MH, Dogan G, Ecemis AS, Arslan HD. School buildings performance in 7.7 Mw and 7.6 Mw catastrophic earthquakes in southeast of Turkey. J Build Eng 2023;79:107810.

[9] Nemutlu ÖF, Balun B, Sarı A. 06 Şubat 2023 Kahramanmaraş Depremleri Kaynaklı Yapısal Hasarların Adıyaman İli Özelinde İncelenmesi. 3rd Int. Conf. Innov. Acad. Stud., Konya, Turkey: 2023, s. 353–61.

[10] Işık E, Avcil F, Arkan E, Büyüksaraç A, İzol R, Topalan M. Structural damage evaluation of mosques and minarets in Adıyaman due to the 06 February 2023 Kahramanmaraş earthquakes. Eng Fail Anal 2023;151.

[11] Büyüksaraç A, Işık E, Bektaş Ö, Avcil F. Achieving Intensity Distributions of 6 February 2023 Kahramanmaraş (Türkiye) Earthquakes from Peak Ground Acceleration Records. Sustain 2024;16.

[12] Nemutlu ÖF, Sarı A, Balun B. 06 Şubat 2023 Kahramanmaraş Depremlerinde (Mw 7.7-Mw 7.6) Meydana Gelen Gerçek Can Kayıpları Ve Yapısal Hasar Değerlerinin Tahmin Edilen Değerler İle Karşılaştırılması. Afyon Kocatepe Univ J Sci Eng 2023;23:1222–34.

[13] Shiwua AJ, Rutman Y. Assessment of Seismic Input Energy By Means of New Definition and the Application To Earthquake Resistant Design. Archit Eng 2016;1.

[14] Çalım F, Güllü A, Yüksel E. Evaluation of Seismic Input Energy Distribution in Moment Frames. 14th Int Congr Adv Civ Eng 2021:1–6.

[15] Manfredi G. Evaluation of seismic energy demand. Earthq Eng Struct Dyn 2001;30:485–99.

[16] Chou C-C, Uang C-M. Establishing absorbed energy spectra-an attenuation approach. Earthq Eng Struct Dyn 2000;29:1441–55.
[17] Hancıoğlu B. Yapıların Deprem Davranışının Enerji Esaslı Analizi. Yıldız Teknik Üniversitesi, 2009.
[18] Decanini LD, Mollaioli F. An energy-based methodology for the assessment of seismic demand. Soil Dyn Earthq Eng 2001;21:113–37.
[19] Erberik A, Sucuoğlu H. Seismic energy dissipation in deteriorating systems through low-cycle fatigue. Earthq Eng Struct Dyn 2004;33:49–67.
[20] Benavent-Climent A. An energy-based damage model for seismic response of steel structures. Pacific Conf Earthq Eng 2007:1–6.
[21] Chai YH. Incorporating low-cycle fatigue model into duration-dependent inelastic design spectra. Earthq Eng Struct Dyn 2005;34:83–96.
[22] Ucar T. Computing input energy response of MDOF systems to actual ground motions based on modal contributions. Earthq Struct 2020;18:263–73.
[23] Kostinakis K, Fontara IK, Athanatopoulou AM. Scalar Structure-Specific Ground Motion Intensity Measures for Assessing the Seismic Performance of Structures: A Review. J Earthq Eng 2018;22:630–65.
[24] Moustafa A, Takewaki I. Characterization of earthquake ground motion of multiple sequences. Earthq Struct 2012;3:629–47.
[25] Kamal M, Inel M. Correlation between ground motion parameters and displacement demands of mid-rise rc buildings on soft soils considering soil-structure-interaction. Buildings 2021;11.
[26] Cao V Van, Ronagh HR. Correlation between seismic parameters of far-fault motions and damage indices of low-rise reinforced concrete frames. Soil Dyn Earthq Eng 2014;66:102–12.
[27] Ozmen HB, Inel M. Damage potential of earthquake records for RC building stock. Earthq Struct 2016;10:1315–30.
[28] Yang D, Pan J, Li G. Non-structure-specific intensity measure parameters and characteristic period of near-fault ground motions Dixiong. Earthq Eng Struct Dyn 2009;38:1257–80.
[29] Elenas A, Meskouris K. Correlation study between seismic acceleration parameters and damage indices of structures. Eng Struct 2001;23:698–704.
[30] Poreddy LR, Pathapadu MK, Navyatha C, Vemuri J, Chenna R. Correlation analysis between ground motion parameters and seismic damage of buildings for near-field ground motions. Nat Hazards Res 2022;2:202–9.
[31] SeismoSoft. SeismoSignal-Signal Processing of Strong Motion Data 2021.
[32] AFAD. 06 Şubat 2023 Pazarcık (Kahramanmaraş) Mw 7.7 Elbistan (Kahramanmaraş) Mw 7.6 Depremlerine İlişkin Ön Değerlendirme Raporu. 2023.
[33] TEC. Turkish Earthquake Code. Ankara, Turkey: 2018.
[34] Yang D, Pan J, Li G. Non-structure-specific intensity measure parameters and characteristic period of near-fault ground motions. Earthq Eng Struct Dyn 2009;38:1257–80.
[35] Riddell R, Garcia JE. Hysteretic energy spectrum and damage control. Earthq Eng Struct Dyn 2001;30:1791–816.
[36] Akkar S, Özen Ö. Effect of peak ground velocity on deformation demands for SDOF systems. Earthq Eng Struct Dyn 2005;34:1551–71.
[37] Chen G, Yang J, Liu Y, Kitahara T, Beer M. An energy-frequency parameter for earthquake ground motion intensity measure. Earthq Eng Struct Dyn 2023;52:271–84.